Inorg. Chem. **2004**, *43*, 2459–2461

Crystallographic Evidence for Chromium–Platinum Interaction

Thomas A. Scott, Besma Abbaoui, and Hong-Cai Zhou*

Department of Chemistry and Biochemistry, Miami University, Oxford, Ohio 45056

Received January 6, 2004

Heteronuclear Pt–Cr paddlewheel complexes with significant Pt–Cr interaction have been made. They can be interconverted. Upon oxidation, the Pt–Cr distance shortens significantly while other bond lengths remain unchanged. By taking into account the strong axial coordination from the chloride ligand in the oxidized compound, we suspect that the removed electron upon oxidation is probably from a Pt–Cr orbital that is significantly antibonding in nature.

In the past 40 years, thousands of compounds containing metal−metal bonds have been synthesized and characterized, the majority of them being homodinuclear species.[1] The main structural motif for this chemistry has been the paddlewheel structure where the metal−metal bond defines the axis, and the four bidentate bridging ligands form the paddles of the paddlewheel.[2] Contrary to the study of homoleptic metal−metal bonds, the research on heterometallic bonding is relatively rare except the study on quadruple bonds, in which case even compounds with unsupported heterobimetallic bonds were made due to the great strength of metal−metal bonding.[3]

Although Cr−Cr bonds and Pt−Pt bonds are common, a Pt−Cr bond has not been explicitly established. In the chromium−platinum compounds that were characterized crystallographically, the Pt−Cr distances range from 2.50 to 2.91 Å.[4] In the work where the shortest Pt−Cr distance was found, no Pt−Cr interaction was identified.[4a] In another work, two $PtMe_2$ moieties were placed at the two axial positions along a Cr−Cr bond, and the bond was lengthened from 2.02 to 2.39 Å.[4b] This elongation was attributed to Pt→Cr dative bonding although a much longer Pt−Cr distance of 2.81 Å was found. The discrepancy between the two reports prompted us to search for the elusive evidence for Pt−Cr interaction. Herein we report three Pt−Cr paddlewheel complexes including the first two Pt−Cr(II) paddlewheel compounds, one of the two being the first Pt−Cr paddlewheel complex without axial coordination.

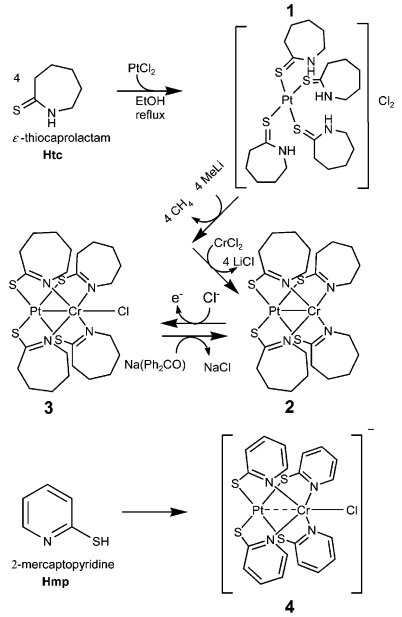

Figure 1. The formation of Pt−Cr heteronuclear complexes.

The reaction scheme and the designation of compounds and abbreviations are given in Figure 1.[5] The design of the experiments is inspired by Cotton's work[1] on homodinuclear complexes and Kinoshita's solvothermo synthesis[4a] of heterobimetallic compounds in toluene.

As Figure 1 shows, the ligand ϵ-thiocaprolactam (Htc) binds a Pt atom through the S atom to form a square planar complex, **1**.[6] Using **1** as a precursor to the formation of a paddlewheel complex has the following advantages: (1) Due to the soft−soft donor−metal combination, the Pt−S bonds

(1) Cotton, F. A.; Walton, R. A. *Multiple Bonds between Metal Atoms*, 2nd ed.; Oxford University Press: New York, 1993.
(2) Cotton, F. A.; Hillard, E. A.; Murillo, C. A.; Zhou, H.-C. *J. Am. Chem. Soc.* **2000**, *122*, 416.
(3) (a) Katović, V.; Templeton, J. L.; Hoxmeier, R. J.; McCarley, R. E. *J. Am. Chem. Soc.* **1975**, *97*, 5300. (b) Garner, C. D.; Senior, R. G.; King, T. J. *J. Am. Chem. Soc.* **1976**, *98*, 3526. (c) Hanson, B. E.; Cotton, F. A. *Inorg. Chem.* **1978**, *17*, 3237. (d) Collman, J. P.; Boulatov, R.; Jameson, G. B. *Angew. Chem., Int. Ed.* **2001**, *40*, 1271. (e) Collman, J. P.; Boulatov, R. *Angew. Chem., Int. Ed.* **2002**, *41*, 3948, and references therein.
(4) (a) Kitano, K.; Tanaka, R.; Kimura, T.; Tsuda, T.; Shimizu, S.; Takagi, H.; Nishioka, T.; Shiomi, D.; Ichimura, A.; Kinoshita, I.; Isobe, K.; Ooi, S. *J. Chem. Soc., Dalton Trans.* **2000**, 995. (b) Mashima, K.; Tanaka, M.; Tani, K. *J. Am. Chem. Soc.* **1997**, *119*, 4307. (c) Powell, J.; Gregg, M. R.; Sawyer, J. F. *Inorg. Chem.* **1989**, *28*, 4451. (d) Bender, R.; Braunstein, P.; Jud, J.-M.; Dusausoy, Y. *Inorg. Chem.* **1984**, *23*, 4489. (e) Howard, J. A. K.; Jeffery, J. C.; Laguna, M.; Navarro, R.; Stone, F. G. A. *J. Chem. Soc., Dalton Trans.* **1981**, 751.
(5) See Supporting Information for experimental procedures, elemental analysis data, and X-ray crystallographic studies for compounds **1**−**4**.
(6) Dini, P.; Bart, J. C. J.; Santoro, E.; Cum, G.; Giordano, N. *Inorg. Chim. Acta* **1976**, *17*, 97−104.

10.1021/ic049968c CCC: $27.50
Published on Web 03/18/2004

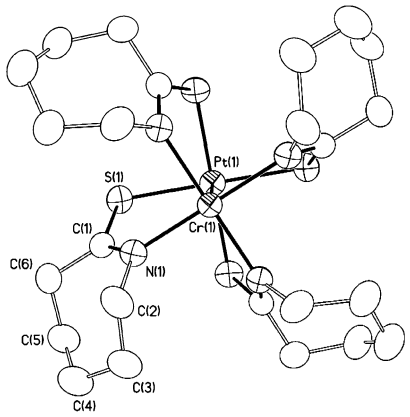

Figure 2. Structure of Δ-[PtCr(tc)$_4$] (**2**) showing 50% probability ellipsoids and partial atom labeling schemes. Hydrogen atoms are omitted for clarity. The Pt−Cr bond resides on a crystallographic 4-fold axis. The crystal is a racemate.

Table 1. Selected Bond Distances (Å), Torsional Angles (deg), and Metal Oxidation States

						oxidation state	
	Pt−Cr	Cr−Cl	Pt−S	Cr−N	tors angle	Pt	Cr
2	2.583(1)		2.330(1)	2.072(2)	22.81	II	II
3	2.532(1)	2.272(3)	2.314(1)	2.100(3)	26.85	II	III
a	2.497(2)	2.341(4)	2.319(4)	2.10(1)	27.95	II	III
4	2.645(1)	2.707(1)	2.313(1)	2.157(2)	26.91	II	II

[a] Reference 4a.

are not labile. This prevents the replacement of the Pt atom by a Cr atom. (2) In **1**, the four nitrogen donor atoms are protected by four protons. When the ligands are deprotonated, there are no unbound Pt atoms around eliminating the formation of a Pt−Pt paddlewheel complex. (3) The square planar geometry of the Pt atom ensures the paddlewheel arrangement when the Cr atom is introduced. (4) Geometric isomers, in which the four bridging ligands orient themselves around the Pt−Cr axis differently (Figure 2), have been avoided. The only product isolated is the isomer with the Pt atom at the S end and Cr at the N end. (5) The aliphatic ring in tc$^-$ enhances solubility of **2** and **3** in benzene allowing the isolation of the product from LiCl formed during the reaction.

Compound **4** has been prepared by taking advantage of the lower solubility in THF of an ionic species supported by the anion of 2-mercaptopyridine (mp$^-$). The ligand mp$^-$ is essentially the same as the anion of 4-methyl-2-mercaptopyridine (mmp$^-$) used by Kinoshita.[4a]

Other than the solubility of the final complex, the ligand tc$^-$ is also geometrically and electronically very similar to ligands mp$^-$ and mmp$^-$. For instance, the C−N and C−S distances and the N−C−S angle of the bridging part of the three ligands do not change significantly.[5]

The crystal structures for **2**, **3**, and **4** are very similar except for the Pt−Cr and Cr−Cl distances. Only the structure of **2** is shown in Figure 2. The relevant bond distances and angles are listed in Table 1.

For comparison, the relevant bond distances and angles of PtCr(mmp)$_4$Cl[4a] are also listed in Table 1.

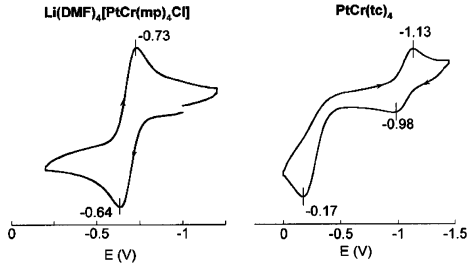

Figure 3. Cyclic voltammograms (100 mV/s) of **4** in 0.1 M (Bu$_4$N)(PF$_6$) solution in DMF and **2** in 0.2 M (Bu$_4$N)(PF$_6$) solution in THF. Peak potentials are those versus Ag/AgCl ($E_{1/2}$ vs Fc: 0.69 V).

Molecules of **2**, **3**, and **4** all reside on crystallographic 4-fold axes. They are all twisted paddlewheels; the S−Pt−Cr−N torsional angles (tors.) are about the same for **3**, **4**, and PtCr(mmp)$_4$Cl,[4a] but that for **2** is slightly smaller due to the absence of the axial ligand.[7] They are all racemic mixtures of two enantiomers with opposite twisting. Although **3** and PtCr(mmp)$_4$Cl[4a] are one electron oxidized, their Pt−S and Cr−N distances are not significantly shorter than those of **2** and **4**. The biggest difference is the distances *along* the Pt−Cr vector.

Compounds **2** and **4** are at the same oxidation state, Pt(II)−Cr(II). However because of the axial coordination in **4**, the Pt−Cr distance is lengthened by 0.062(1) Å, reminiscent of the well-known sensitivity of the Cr−Cr quadruple bonds to axial coordination.[8] The electrochemistry of the two compounds is also different. Compound **2** has a quasireversible redox pair at $E_{1/2} = -1.06$ V (Figure 3). Compound **4** has a reversible wave at $E_{1/2} = -0.69$, which is different from the literature value for PtCr(mmp)$_4$Cl.

Chemical oxidation of **4** did not yield single crystals of [PtCr(mp)$_4$Cl] due to solubility problems, but the existence of PtCr(mmp)$_4$Cl[4a] showed the feasibility of the chemical oxidation.

Ignoring the small difference between the two ligands mp$^-$ and mmp$^-$, going from **4** to PtCr(mmp)$_4$Cl,[4a] a positive charge is added to the Pt−Cr core; one would expect bigger electrostatic repulsion between the two metal atoms thus causing a longer Pt−Cr separation.[9] However, the Pt−Cr distance is *shortened* from 2.645(1) Å in **4** to 2.497(2) Å in PtCr(mmp)$_4$Cl[4a] by 0.148(2) Å. What is more astonishing is that in PtCr(mmp)$_4$Cl[4a] the axial coordination, the major factor known for the elongation of Cr−Cr bonds,[10] is a lot stronger: the Cr−Cl distance is 2.341 (4) Å in PtCr(mmp)$_4$Cl[4a] but 2.707(1) Å in **4**. This remarkable shortening of Pt−Cr distance despite strong axial coordination strongly suggests that, going from **4** to PtCr(mmp)$_4$Cl,[4a] the electron that is removed is probably from a Pt−Cr antibonding orbital.

More evidence for this remarkable shortening comes from the oxidation of **2** to **3**. When **2** was oxidized by ferrocenium

(7) Clérac, R.; Cotton, F. A.; Daniels, L. M.; Dunbar, K. R.; Murillo, C. A.; Zhou, H.-C. *Inorg. Chem.* **2000**, *39*, 3414.
(8) Cotton, F. A.; Daniels, L. M.; Murillo, C. A.; Pascual, I.; Zhou, H.-C. *J. Am. Chem. Soc.* **1999**, *121*, 6856.
(9) Cotton, F. A.; Murillo, C. A.; Zhou, H.-C. *Inorg. Chem.* **2000**, *39*, 3261.
(10) Cotton, F. A.; Daniels, L. M.; Murillo, C. A.; Zhou, H.-C. *Inorg. Chim. Acta* **2000**, *300*−*302*, 319.

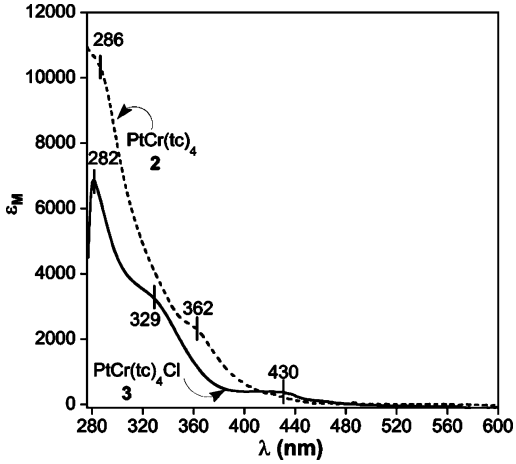

Figure 4. Absorption spectra of [$PtCr(tc)_4$] and [$PtCr(tc)_4Cl$] in THF.

hexafluorophosphate in the presence of LiCl, the one electron oxidized product **3** was obtained. Compound **3** has also been reduced chemically with the concomitant loss of the axial ligand to form **2**. Going from **2** to **3**, the Pt−Cr distance shortened despite a very strong axial coordination from a Cl^- anion (Cr−Cl distance is as short as 2.272(3) Å).

Absorption spectra of **2** and **3** are set out in Figure 4. The spectrum of compound **2** has no feature in the visible region other than a steady increase in absorptivity going into the UV range. This is consistent with the pale yellow color of **2** in THF. Measurement at higher concentration is not accessible due to limited solubility of **2** in THF (1.3×10^{-3} mol·L^{-1}) and in other common organic solvents. The absorption spectrum of **3** shows a band at 430 nm, and the molar absorptivity is 3.65×10^2 L·mol^{-1}·cm^{-1}. The color of the solution of **3** in THF is greenish yellow, but the crystals of **3** are green in color. This is different from $PtCr(mmp)_4Cl$,[4a] which was described as an orange-red crystalline solid although in both compounds the oxidation states and coordination environments of metal atoms are identical.

The EPR signal of **3** shows characteristics of an $S = {}^3/_2$ ground state, which is consistent with the magnetic susceptibility measurement of $PtCr(mmp)_4Cl$.[4a] Magnetic susceptibility measurement of **2** reveals four unpaired electrons.

On the basis of the EPR spectrum and magnetic susceptibility measurement, a schematic MO diagram can be drawn (Figure 5). The twisting of the paddlewheel in both compounds **2** and **3** lowers their symmetry from C_{4v} to C_4. This will only affect the δ bonding, which is not important at a current metal−metal distance of 2.5 Å. On the other hand, the strength of the π and σ bonding will not change whether the paddlewheel is twisted or not. To simplify the molecular orbital treatment, C_{4v} point group symmetry will be used for both **2** and **3**.

The interactions among the E (d_{xz}, d_{yz}) and B_2 (d_{xy}) orbitals (π and δ bonding) will be minor due to the long metal−metal separation. However, σ interaction between the metal A_1 (d_{z^2}) orbitals cannot be ignored because the d_{z^2} orbitals are more extended along the bonding axis.

On the left of Figure 5, the interaction between a square planar $Cr^{II}N_4$ unit and a square planar PtS_4 unit is shown.

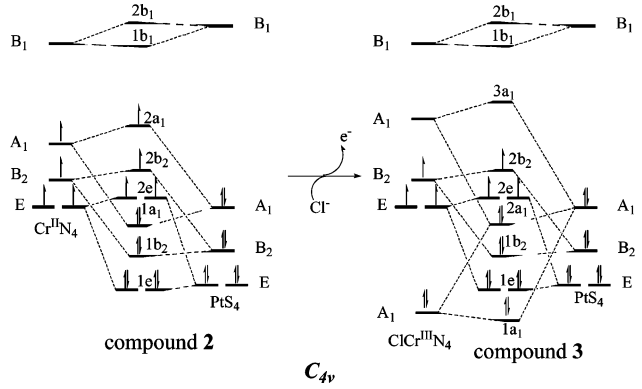

Figure 5. Schematic MO diagram showing the Pt−Cr interaction.

Ignoring the π and δ interactions, the net bond order in **2** is 0.5 (σ bonding). On the right, the Pt−Cr interaction between a square pyramidal $ClCr^{III}N_4$ unit and a square planar PtS_4 unit is given. Despite the destabilization of the Cr A_1 (d_{z^2}) orbital by Cr−Cl bonding, the bond order increases to 1 in compound **3**.

Another way to look at the Pt−Cr interaction is to view the Pt atom as a "ligand" with a lone pair in its d_{z^2} orbital to interact with the d_{z^2} orbital of the Cr atom (Pt→Cr dative interaction). When the Cr d_{z^2} orbital is half-occupied, the $Pt-Cr^{II}$ interaction is weak, but when this orbital is empty, the $Pt-Cr^{III}$ interaction is much stronger.

The schematic MO diagram in Figure 5, although crude, explains the shortening of the Pt−Cr distances upon oxidation despite the bond lengthening from the axial coordination of the chloride anion. It is also consistent with the absorption spectra, EPR study, and magnetic susceptibility measurement. To obtain a refined MO diagram, theoretical calculations are now being carried out in Dr. Michael B. Hall's lab at Texas A&M University. The synthesis of a $Pt-Cr^{III}$ paddlewheel compound without axial coordination is currently underway in our lab. If successful, it should provide further evidence for the intriguing Pt−Cr interaction.

In summary, we have prepared Pt−Cr(II) paddlewheel complexes for the first time and found strong crystallographic evidence for Pt−Cr interaction.

Acknowledgment. We thank Sara L. Milam and Chris Behm for experimental assistants, John F. Berry for the magnetic susceptibility measurement, Nathan F. Wenzel for assistance in EPR study, and Professors F. Albert Cotton, Carlos A. Murillo, and Michael B. Hall for discussion. We thank Miami University and the donors of the American Chemical Society Petroleum Research Fund for financial support. H.-C.Z. also thanks the Research Corporation for a Research Innovation Award. The X-ray diffractometer is supported by NSF Grant EAR-0003201.

Supporting Information Available: Experimental procedure, elemental analysis data, and crystallographic data for compounds **1**−**4** (CIF). This material is available free of charge via the Internet at http://pubs.acs.org.

IC049968C